Profiling of Vascular Endothelial Growth Factor Receptor Heterogeneity Identifies Protein Expression-defined Subclasses of Human Non-small Cell Lung Carcinoma

TIMOTHY R. HOLZER[1*], ANGIE D. FULFORD[1], LESLIE O'NEILL REISING[1], DREW M. NEDDERMAN[1], XUEKUI ZHANG[2], LAURA E. BENJAMIN[3], ANDREW E. SCHADE[1] and AEJAZ NASIR[1]

[1]Diagnostic and Experimental Pathology, [2]Oncology Statistics, and [3]Cancer Biology and Angiogenesis, Lilly Research Laboratories, Eli Lilly and Company, Lilly Corporate Center, Indianapolis, IN, U.S.A.

Abstract. *Background: the vascular endothelial growth factor (VEGF) pathway plays a prominent role in the growth and progression of human cancer, including non-small cell lung carcinoma (NSCLC). The key mediators of VEGF signaling are a family of related receptor tyrosine kinases that include VEGFR1, VEGFR2, and VEGFR3. The relative expression levels, activity, and cross-talk among these receptors may contribute to response of NSCLC to anti-angiogenic therapies, and a better systematic, translatable approach to categorizing tumors is needed. Materials and Methods: We comparatively evaluated immunohistochemical expression of the three VEGFRs in archival primary NSCLC tissues (n=96). Results: VEGFR1 and VEGFR2 were localized both in vessels and tumor cells, while VEGFR3 was only localized in tumor vessels. A set of eight VEGFR staining subclasses were identified: Triple VEGFR positive (n=11, 11.5%), VEGFR1 predominant (n=22, 22.9%), VEGFR2 predominant (n=9, 9.4%), VEGFR3 predominant (n=3, 3.1%), VEGFR1/2 predominant (13, 13.5%), VEGFR1/3 predominant (2, 2.1%), VEGFR2/3 predominant (n=8, 8.3%), and triple VEGFR negative (n=28, 29.2%). An objective categorization based on K-means clustering revealed four clusters, three of which showed high VEGFR2 compared to VEGFR3 (30.7% of cases), cases high in both VEGFR2 and VEGFR3 (18.2%), and cases that were negative/low for both VEGFR2 and VEGFR3 (45.4%). A positive association between VEGFR2 and VEGFR3 was found, however no associations were observed between VEGFR1 and VEGFR2, nor VEGFR1 and VEGFR3. Conclusion: The proposed subclasses of NSCLC are an approach for complementing lines of investigation of anti-angiogenic therapies beginning with systematic characterization of the disease.*

Correspondence to: Timothy R. Holzer, Ph.D., Eli Lilly and Company, Lilly Corporate Center, DC0438, Indianapolis, IN 46285, U.S.A. Tel: +1 3172776369, e-mail: holzertr@lilly.com and Aejaz Nasir, MD, MPhil, FCAP, Eli Lilly and Company, Lilly Corporate Center, DC0424, Indianapolis, IN 46285, U.S.A. Tel: +1 3176515535, e-mail: nasirae@lilly.com

Key Words: VEGFR, VEGFR1, VEGFR2, VEGFR3, non-small cell lung cancer, lung cancer, NSCLC, immunohistochemistry.

The molecular mechanisms of angiogenesis are exploited by numerous human cancer types to stimulate tumor growth and progression (1, 2). These include cancer of the lung, the leading cause of cancer death worldwide (3, 4). In non-small cell lung carcinoma (NSCLC), several anti-angiogenic agents have shown clinical efficacy in various histological subtypes (5-9), however NSCLC continues to be one of the most frequent and aggressive forms of human cancer (10, 11). In order to better understand and to target resistance to anti-angiogenic mechanisms, an improvement in reliable characterization of the most appropriate biomolecular factors that govern the complex architecture of angiogenic signaling in NSCLC may be needed (12).

Many factors work in concert to elicit effects on angiogenic processes, but the most prominent factors are vascular endothelial growth factor (VEGF) and its cognate receptor, VEGF receptor 2 (VEGFR2) (2, 13). VEGFR2 belongs to a class of receptor tyrosine kinases exhibiting seven immunoglobulin-like domains in their extracellular regions (type V) and includes family members VEGFR1 and VEGFR3 (14). These receptors are commonly located in the vascular and lymphatic endothelium within tumor stroma and are involved in the differentiation, maintenance, proliferation, and/or migration of endothelial cells (15, 16). A number of studies have evaluated expression of the VEGFRs with or without parallel assessment of vascular density and various VEGF ligands in NSCLC tissues (17). These include more focused analyses of the VEGFA growth factor and its two receptors,

VEGFR1 and VEGFR2 (18), as well as profiling of VEGFC and/or VEGFR2 and VEGFR3 in the tumor vasculature (19-22). While individual VEGFRs have been shown to have prognostic relevance (23), systematic analysis of vascular expression of the three VEGFRs using a quantifiable scoring approach has not been uniformly applied in these studies.

Recently, we implemented immunohistochemical (IHC) assays for two members of the VEGFR family following a rigorous development paradigm (24, 25). Here, we developed an IHC for a third VEGFR family member and applied these assays to an independent series of archival primary NSCLC with the following aims: i) characterization of the heterogeneity of IHC-based expression of the three VEGFRs in NSCLC tissues, ii) determination of associations among the prevalence of these three VEGFRs in NSCLC, and iii) identification of prominent subsets of patients with NSCLC based on relative expression of the three VEGFRs. As the relative expression and interaction among these receptors may allow a better understanding of the intricacies of VEGF signaling, we propose this systematic VEGFR protein profiling approach to complement established disease characterization methodologies in NSCLC (26).

Materials and Methods

Human tissue specimens. Commercially available human tumor tissue microarrays (TMAs) were purchased from TriStar Technology Group (Rockville, MD, USA) for this study. Use of human tissues in this study followed standard operating procedures of TriStar, and considered informed donor consent, Institutional Review Board approval, patient anonymity, compliance with current international and European Union regulations.

A human NSCLC TMA comprising samples from 111 patients was made from formalin-fixed paraffin-embedded (FFPE) tissue blocks collected by a standard procedure that considered tissue preservation (TriStar). Clinical data were reviewed by team of pathologists and oncologists. Under supervision of qualified consultant pathologists, NSCLC tissues were collected from surgically resected primary tumor tissues from adult patients, processed, and used to construct TMAs. A single 1 mm core was obtained from the most representative area of the donor block from each patient. The selection of cases represented a random sample of various histopathological subtypes, histological grades and stages of NSCLC. Each case was histologically typed by the Tristar Pathologists, based on the histopathological criteria proposed in the World Health Organization (WHO) Classification of Lung Tumors (27, 28). The hematoxylin and eosin-stained TMA slide was also reviewed by a board-certified anatomic pathologist (AN) for confirmation of histopathological diagnoses and to update the submitted diagnoses of bronchioloalveolar carcinomas (n=5) to adenocarcinoma (ADC) with lepidic pattern, using the latest (2015) WHO criteria (27, 28). Any cores featuring equivocal histology, technical failure, attrition of sampled cores, or which had missing clinicopathological data (*e.g.* demographic information) were excluded, resulting in 96 evaluable NSCLC specimens. Patients were followed-up for up to 14 years or until death. Clinicopathological characteristics of patients and their specimens are summarized in Table I. For VEGFR3 assay development, additional human tumor blocks were obtained from commercial sources (Asterand, Detroit, MI, USA; and Tristar), including angiosarcoma, and colonic adenocarcinoma (CRC) specimens. Acquisition and processing of these tissues was confirmed to be in line with rigorous human tissue-acquisition protocols that ensure collection and supply of quality human tissues for novel biomarker studies. Asterand states that collaborators obtained the following: approval of institutional and independent review board, authorization from a privacy officer, and necessary government licenses and industry accreditations. Informed consent documentation used by Asterand was subjected to review and approval by regulatory and ethics authorities. If necessary, Asterand obtained a waiver of informed consent from an institutional review board to enable the use of the tissues and clinical information for exploratory research.

Cell culture and processing of cell lines. All cells were obtained from the American Type Culture Collection (Manassas, VA, USA). All media were supplemented to include 1% (v/v) penicillin/streptomycin and 10% fetal bovine serum (FBS). HEL (erythroleukemia) cells were expanded using RPMI-1640 with 10 mM HEPES, and 1 mM sodium pyruvate. A549 (lung carcinoma) cells were propagated with F-12K medium. U87MG (glioblastoma) with Eagle's minimum essential medium with Earle's balanced salt solution supplemented with both 0.5 mM sodium pyruvate and 1% non-essential amino acids. All cells were propagated at 37˚C and 5% CO_2, then harvested by incubation in 0.25% trypsin with 0.53 mM EDTA at 37˚C, and then collected by pipetting. Cells were pooled and then aliquoted for: i) paraffin embedding by fixation in 10% neutral buffered formalin (NBF) for 24 h, or ii) western blotting by pelleting and lysing as described below. Histotechnological preparation of cell lines was performed as described previously (24).

Western blots. Whole-cell extracts were prepared by re-suspending in protease and phosphatase inhibitor-supplemented RIPA buffer (Thermo Scientific, Waltham MA, USA). Jurkat (acute T-cell leukemia) whole cell lysate was included (Abnova, Walnut, CA, USA). Samples were combined with loading buffer containing sodium dodecyl sulfate and dithiothreitol, placed in a 95˚C heat block for 3 min, and then separated on NuPage 4-12% bis-tris polyacrylamide gels (Thermo Scientific). Recombinant proteins were added as controls: a dilsufide-linked homodimer of VEGFR3 N-terminal region/Fc chimera (P35916_a.a. 25-776 plus 473-776; R&D Systems, Minneapolis, MN, USA; rECD-A) and HIS-tagged *N*-terminal region of VEGFR3 (NP_002011.2_a.a. 1-775; rECD-B) produced by transient transfection, then purified on nitrilotriacetic acid affinity and size-exclusion chromatography columns. Gels were transferred to nitrocellulose membranes and probed with a primary antibody to VEGFR3 (9D9F9; EMD Millipore, Billerica, MA, USA) overnight at 4˚C with agitation. Blots were incubated with species-specific, horseradish peroxidase-conjugated secondary antibodies for 1 h then visualized using enhanced chemiluminescence detection (Pierce, Thermo Scientific). A glyceraldehyde 3-phosphate dehydrogenase-directed primary antibody (clone 14C10; Cell Signaling Technologies, Danvers, MA, USA) was used to verify equal protein loading on gels. All primary antibodies were applied at a working dilution of 1:1000.

Immunohistochemistry. We developed and optimized specific and selective assays for evaluation of VEGFR1, VEGFR2, and VEGFR3 in archival human tissues. Staining methodologies for VEGFR1 (using a rabbit monoclonal IgG, 1303-1; Abcam/Epitomics,

Table I. *Clinicopathological characteristics of evaluable cases in non-small cell lung carcinoma cohort (TA1249, n=96).*

Characteristic	Value
Mean age (range), years	65 (40-78)
Gender, n (%)	
Male	80 (83.3%)
Female	16 (16.7%)
Race, n (%)	
White	96 (100%)
Histopathological subtype, n (%)	
ADC	37 (40.6%)
Squamous cell	39 (41.1%)
Bronchioloalveolar*	5 (5.2%)
Large cell, undifferentiated	7 (7.3%)
Adenosquamous	2 (2.1%)
Other mixed	3 (3.1%)
NOS	3 (3.1%)
AJCC 2006 stage, n (%)	
IA/IB	57 (59.4%)
IIA/IIB	19 (19.8%)
IIIA/IIIB	19 (19.8%)
IV	1 (1.0%)
Median overall survival (range), months	0.2-168 (60.2)

ADC: Adenocarcinoma; NOS: not otherwise specified; AJCC: American Joint Committee on Cancer (46). *ADC with lepidic pattern (28).

Burlingame, CA, USA) and VEGFR2 (using a rabbit monoclonal IgG, 55B11; Cell Signaling Technologies) IHC were performed as previously described (24, 25, 29). To detect VEGFR3, FFPE sections of the NSCLC TMA were cut, dried, and then baked at 60˚C prior to staining. Slides were deparaffinized and rehydrated on the Bond III automated stainer (Leica Biosystems, Buffalo Grove, IL, USA), and antigens were retrieved at 100˚C for 40 min in EDTA-based buffer at pH 9 (ER2). Endogenous peroxidases were treated with peroxide block for 5 min, and then a protein block (PowerVision Super Block; Leica Biosystems) was applied for 10 min. Anti-VEGFR3 mouse monoclonal IgG (clone 9D9F9; Millipore) was applied at ~1.0 μg/ml (based on a 1:3000 dilution of stock ascites fluid) in antibody diluent for 15 min. A post-primary reagent (Leica Biosystems) was applied for 8 min to enable detection of mouse primary antibodies. Refine HRP Polymer (Leica Biosystems) was next applied for 8 min, 3,3'-diaminobenzidine (DAB Refine Chromogen; Leica Biosystems) was applied for 10 min, and then slides were counterstained with hematoxylin for 5 min. Slides were removed from the stainer, dehydrated by sequential submersion in 95% ethanol, 100% ethanol, and xylene, and coverslipped following routine procedures. Reagent negative controls and isotype-specific IgG were used to assess non-specific staining for each tissue. Serial sections of tissues were stained at a Clinical Laboratory Improvement Amendments-certified reference lab (Clarient, Aliso Viejo, CA, USA) using the well-established IHC assay protocols for podoplanin (D2-40), and CD34 (QBEnd/10), for lymphatic and blood vessels, respectively (30, 31). To represent various individual or combined VEGFR staining patterns, images were obtained from high-resolution digital scans at ×200 original magnification (Scanscope XT; Aperio Technologies, Vista, CA, USA).

Pre-absorption assays. For initial selectivity assays, *N*-terminal/Fc chimera recombinant proteins for VEGFR1 (AAC50060_a.a. 27-687), VEGFR2 (AAC16450_ a.a. 20–764), and VEGFR3 (rECD-A, as above) were obtained from R&D Systems. When performing pre-absorption assays, the diluted anti-VEGFR3 was combined with a 25-fold molar excess of recombinant proteins in antibody diluent. Mixtures were incubated overnight (12-15 h) at 4˚C with rocking before application in IHC.

Brightfield in situ hybridization (BRISH). FFPE sections were cut and dried as described above and used for automated BRISH. Dry slides were loaded on a Bond RX instrument (Leica Biosystems), and deparaffinization, rehydration, and pre-treatment using EDTA buffer solution (ER2, pH 9; Leica Biosystems) was performed at 100˚C for 15 min for FFPE cell lines and tumor tissues. RNAscope LS reagent kit (Advanced Cell Diagnostics, Hayward, CA, USA) was then used for detection of mRNA. Briefly, protease was applied for 20 min at 40˚C, then peroxide was applied for 10 min. *FLT4* (VEGFR3) RNAscope LS probe 2.0 (Advanced Cell Diagnostics) was hybridized at 40˚C for 2 h. The signal amplification steps were performed per manufacturer's instructions for amplifications 1-6, with the addition of a 2× saline sodium citrate stringency wash performed after the first amplification. DAB and hematoxylin were applied as part of the modified Bond Polymer Refine Detection kit (Leica Biosystems). Slides were dehydrated and coverslipped as described above.

Interpretation of IHC. Stained TMA slides were evaluated by a Board-certified pathologist (AN). For each evaluable TMA core, based on unequivocal results, vascular VEGFR1 immunoreactivity was interpreted as present (based on the presence of any number of VEGFR1-positive vessels in tumor stroma) or absent. Tumor cell VEGFR1 expression was interpreted as negative, low, medium, or high based on the intensity and proportion of stained tumor cells. For VEGFR2 positivity in tumor cells, a core was considered positive if at least 50% of the cells exhibited weak, moderate or strong immunoreactivity. For both VEGFR2 and VEGFR3, the numbers of tumor stromal vessels showing unequivocal positive immunoreactivity were counted in each TMA core. Medians and 25th and 75th percentiles for the range of non-zero values for IHC-positive tumor stromal vessel counts were determined for VEGFR2 and separately for VEGFR3. Based on the 25th percentile as the cutoff between low and medium values and the 75th percentile as the cutoff between medium and high values, vascular VEGFR2 counts were categorized as negative/low (≤2 VEGFR2-positive vessels/TMA core), medium (3-10 VEGFR2-positive vessels/TMA core), and high (>10 VEGFR2-positive vessels/TMA core). Similarly, VEGFR3 vessel counts were categorized as negative/low (≤1 positive vessels/TMA core), medium (2-9 positive vessels/TMA core), and high (>9 positive vessels/TMA core). Since tumor cell expression of VEGFR1, when present, was widespread in a given NSCLC tissue while vascular expression of VEGFR1 was variable and frequently focal, we utilized tumor cell expression of VEGFR1 along with vascular expression of VEGFR2 and VEGFR3 in determining the final VEGFR profiles of NSCLC cases in this study.

For determination of subclasses, scores were dichotomized into either positive (medium or high categories) or low/negative. Predominance was defined as positive for one or two VEGFRs and low/negative for the remainder.

The 3-Venn diagram was generated using euler*APE* software (32).

Statistical methods. Associations were determined among the IHC expression levels (negative/low, medium, and high) of the three VEGFRs. The histological subtypes of NSCLC cases (n=88) included in these association analyses were ADC, squamous cell carcinoma (SCC), ADC with lepidic pattern, and large cell carcinoma. VEGFR2 and VEGFR3 were dichotomized as positive (count>0) and negative (count=0). Pearson's chi-squared test was performed on categorical values for VEGFR2 *vs*. VEGFR3. For VEGFR1 *vs*. VEGFR2 and VEGFR1 *vs*. VEGFR3, Fisher's exact test was performed. Since in examining the associations among VEGFRs we conducted these three hypothesis tests, a statistically significant p-value was corrected for multiplicity to be $p<0.0167$ (*i.e*. 0.05/3). Additionally a correlation test (Pearson product-moment) was performed on original, continuous expression scores for VEGFR2 and VEGFR3.

To find any association between expression of VEGFR1, VEGFR2, or VEGFR3 and histology, permutation testing based on 10000 random permutation samples was performed. Preliminary observations on association with histological subtypes found no association for VEGFR1 (permutation Fisher's exact $p=0.48$), marginal association for VEGFR2 (permutation Wilcoxon $p=0.09$), and strong association for VEGFR3 (permutation Wilcoxon $p=0.01$). Based on these findings, an objective form of clustering analysis (K-means) was carried out, using relative vascular expression levels of VEGFR2 and VEGFR3 as a continuous variable. This analysis was based on log-transformed values for VEGFR2- and VEGFR3-positive vascular counts. To determine the number of clusters and control overfitting to noise, Bayesian Information Criteria (BIC) was used to compare multiple models. Our model selection, which was based on best BIC values, resulted in four clusters.

The VEGFR1 expression levels (negative, low, medium and high) were recoded as 1, 2, 3, and 4, respectively, then log-transformed. Based on the availability of analyzable data for all three VEGFRs in the TMA, VEGFR expression values (n=88) were standardized to zero-mean and unit standard deviation and plotted as a heatmap. NSCLC cases with mixed, not otherwise specified (NOS), and adenosquamous histology were excluded from clustering analysis due to the small numbers of cases.

Results

Performance verification of VEGFR3 IHC. Following a comprehensive assay development paradigm, we demonstrated the specificity, selectivity, and appropriate immunoreactivity pattern of VEGFR3 IHC using a similar approach as reported for VEGFR1 and VEGFR2 IHC (24, 29). The mouse monoclonal IgG was first profiled by immunoblot (Figure 1A). In HEL cell lysates, bands were observed at approximately 195 kDa and 130 kDa, consistent with expected molecular weights of uncleaved and cleaved receptor, respectively (33). No bands were observed in lysates from Jurkat, U87MG, or A549 cell lines. Consistent with the results of the western blot, VEGFR3 immunoreactivity was absent in FFPE U87MG cells and positive in HEL cells, showing cytoplasmic and membranous localization (Figure 1B). Dilution of the primary antibody resulted in a decrease of immunoreactivity, and conversely an increase resulted in greater immunoreactivity and possible saturation of the signal. This suggests the selected antibody concentration used was within the linear range of detection. In FFPE human CRC tissue and in squamous cell carcinoma of the lung, VEGFR3 was restricted to the vasculature, consistent with localization of *FLT4* (VEGFR3) mRNA (Figure 1C). Recombinant proteins representing the extracellular domains of VEGFR1 and VEGFR2 failed to abolish immunoreactivity of the VEGFR3 antibody in angiosarcoma tissues, suggesting that it did not cross-react with the other VEGFR family members (Figure 1D). Finally, in CRC, VEGFR3 immunoreactivity was observed in D2-40-positive vessels as well as CD34-positive/D2-40-negative vessels, consistent with the observation that VEGFR3 is expressed in both blood and lymphatic vessels (Figure 1E). After confirming the performance of the VEGFR3 IHC assay, we expanded our analyses into a larger cohort of NSCLC tissues, along with IHC for VEGFR1 and VEGFR2.

VEGFR expression in NSCLC. The results of IHC expression scoring and representation of VEGFR expression heterogeneity are shown in Figure 2. Immunoreactivity for VEGFR1 was localized mainly to tumor cell cytoplasm, tumor stromal vasculature, and, where present, macrophages. Forty-eight out of 96 cases (50.0%) were positive for tumor cell expression of VEGFR1, while 87 cases (90.6%) cases were positive for vascular expression. Overall, when present, tumor cell expression of VEGFR1 was distinct, widespread and diffuse with a given case (core) of NSCLC, while vascular expression was more variable, focal and at times weak in intensity. Out of the 10 cases that were negative for vascular VEGFR1 expression, six were positive for VEGFR1 expression in the tumor cells. Because of the unique expression patterns of VEGFR1 compared to VEGFR2 and VEGFR3, we decided to represent cases as VEGFR1-positive based on an assessment of cytoplasmic expression in tumor cells. Of the cases that were VEGFR1-positive in tumor cells, 33 out of 48 (68.8%) showed a moderate level of expression and 15 (31.3%) a high level. There was no apparent association between VEGFR1 and expression of the other receptors. Out of cases that were negative/low for VEGFR1 (n=48), 17 (35.4%) and 11 (22.9%) expressed VEGFR2 and VEGFR3, respectively.

Immunoreactivity for VEGFR2 was localized mainly in tumor stromal vasculature, with variable expression in tumor cells (17.7% of cases positive). Forty-one cases (42.7%) were positive for vascular VEGFR2 expression.

Twenty-four NSCLC cases (25.0%) were positive for vascular VEGFR3 expression. A representation of the distribution of VEGFRs among all cases is shown in Figure 3. As observed in CRC (Figure 1), immunoreactivity for VEGFR3 in NSCLC was localized exclusively to tumor stromal vasculature, including both lymphatic vessels and blood vessels.

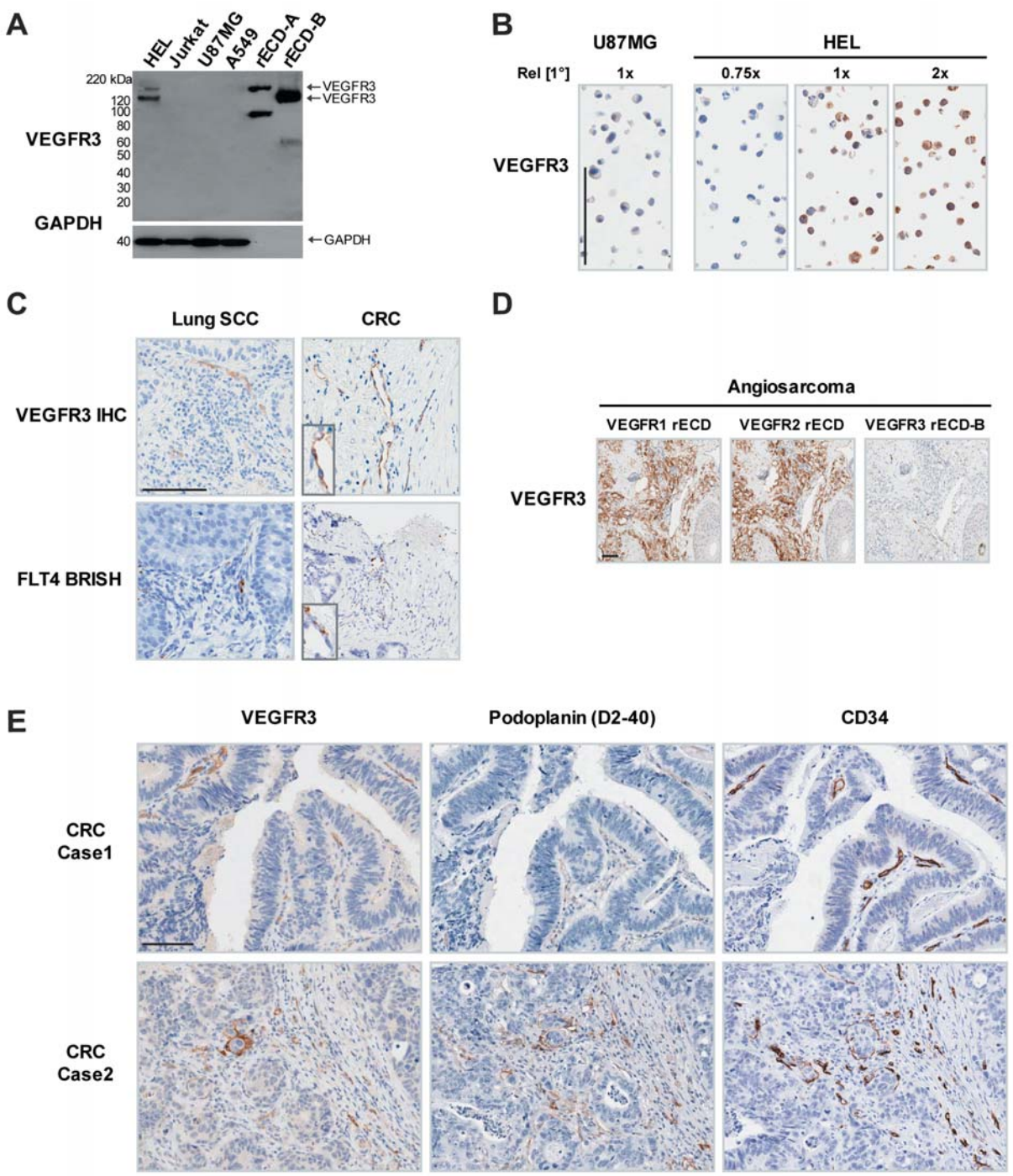

Figure 1. *An optimized immunohistochemistry (IHC) assay reliably detects vascular endothelial growth factor receptor 3 (VEGFR3) protein levels in formalin-fixed, paraffin-embedded tissues and cell lines. A: Immunoblot probed with the anti-VEGFR3 shows a bands at the expected molecular weights (first lane). Recombinant proteins harboring regions of the extracellular domain of VEGFR3 (rECDs) were included as controls. B: VEGFR3 IHC on FFPE versions of cells shows immunoreactivity levels (brown) consistent with the immunoblot. Relative primary antibody concentrations are shown with 1× representing dilution described in Materials and Methods. C: Representative VEGFR3 IHC in human tumor specimens show immunoreactivity in endothelial cells and is consistent with mRNA localization by in situ hybridization. Magnified areas of positive vasculature of colorectal carcinoma (CRC) are shown in insets. D: Pre-absorption assays suggest that VEGFR3 IHC does not cross-react with other VEGFR family members. E: VEGFR3 expression was observed in both CD34-positive blood vessels and podoplanin-positive lymphatic vessels in colorectal adenocarcinoma. Slides were counterstained with hematoxylin (blue). GAPDH: Glyceraldehyde 3-phosphate dehydrogenase; FLT4 BRISH: brightfield in situ hybridization (BRISH) for Fms-related tyrosine kinase 4 mRNA; SCC: squamous cell carcinoma. Original magnification of all IHC and BRISH panels, ×200. Scale bars: 100 μm.*

Case	VEGFR1 endothelium	VEGFR1 tumor cells	VEGFR2+ vessels	VEGFR3+ vessels	Subclass
1	P	L	7	10	VII
2	P	L	0	0	VIII
4	P	L	1	0	VIII
5	P	L	28	14	VII
6	P	L	12	6	VII
7	P	M	0	0	II
8	P	L	8	3	VII
9	P	M	18	10	I
10	P	L	5	5	VII
11	P	M	0	1	II
12	P	M	17	4	I
13	N	H	7	4	I
14	P	L	3	0	III
15	P	M	0	0	II
16	P	M	0	0	II
17	P	M	6	0	V
18	P	H	6	0	V
19	P	M	0	0	II
21	P, F	H	1	0	II
22	P	H	0	1	II
23	P	M	5	0	V
24	P	L	0	0	VIII
25	P, F	L	0	0	VIII
26	P	M	0	0	II
27	P	L	11	0	III
28	P	L	0	7	IV
29	P	M	0	0	II
30	P	M	0	0	II
31	P	L	23	0	III
32	P	M	10	4	I
33	P	H	0	0	II
34	P	N	0	0	VIII
36	P	M	0	6	VI
37	P	M	29	20	I
38	N	M	10	12	I
39	P	L	14	1	III
40	P	L	0	0	VIII
41	P	M	25	7	I
42	N	M	3	4	I
43	P	L	0	0	VIII
44	N	H	2	0	II
46	P	L	0	0	VIII
47	P	H	0	0	II
48	P	L	0	0	VIII
49	P	L	0	3	IV
50	P	M	3	0	V
51	P	H	0	0	II
52	N	L	4	4	VII
53	P	M	16	0	V
54	P	L	2	0	VIII
55	P	L	0	0	VIII

Case	VEGFR1 endothelium	VEGFR1 tumor cells	VEGFR2+ vessels	VEGFR3+ vessels	Subclass
56	P	H	1	0	II
57	P	H	0	0	II
58	P	H	0	0	II
59	P	L	0	0	VIII
60	P	L	0	0	VIII
62	P	L	0	0	VIII
63	N	L	17	4	VII
64	P	L	0	0	VIII
65	P	L	0	0	VIII
66	N	L	2	0	VIII
67	P, F	N	4	0	III
70	P	M	2	0	II
71	P	H	7	0	V
73	P	L	0	10	IV
75	P	M	0	0	II
76	P	L	0	0	VIII
78	P	L	0	0	VIII
79	P	N	3	3	VII
80	P	L	3	0	III
82	P	L	0	0	VIII
83	P	L	0	0	VIII
84	P	L	0	0	VIII
85	N	H	15	2	I
88	P	M	3	0	V
89	P	L	0	0	VIII
91	N	L	2	0	VIII
92	N	L	2	0	VIII
93	P	L	3	0	III
94	P	M	10	0	V
96	P	M	0	0	II
97	P	L	2	0	VIII
98	P	M	0	2	VI
99	P	M	5	2	I
100	P	L	2	0	VIII
101	P	M	3	0	V
102	P	H	0	0	II
103	P	H	0	0	II
104	P	M	3	1	V
105	P	L	13	0	III
106	P	M	8	0	V
107	P	M	4	0	V
108	P	M	8	4	I
109	P	M	11	0	V
110	P	L	7	0	III
111	P	L	0	0	VIII

Color key: Neg/Low | Medium | High

Figure 2. *Color-coded list of immunohistochemical expression of vascular endothelial growth factor receptors (VEGFRs) (1, 2, and 3) in non-small cell lung carcinoma. Vascular VEGFR1 expression (P, positive; N, negative; F, focal) based on any number of tumor stromal vessels showing unequivocal immunoreactivity for VEGFR1 protein. VEGFR1 expression in tumor cells, based on intensity and proportion of stained cells (H, high; M, moderate; L, low; N, negative). VEGFR2 vessel counts were categorized as negative/low (≤2 positively stained), medium (3-10 positively stained), and high (>10 positively stained). VEGFR3 vessel counts were categorized as negative/low (≤1 positively stained), medium (2-9 positively stained), and high (>9 positively stained). Representative cases shown in subsequent figures are marked in red.*

Classification of NSCLC cases based on VEGFR profiling. In line with a previous approach (25), the NSCLC cases were grouped into eight different subclasses based on relative (negative/low, medium, high) expression of the three VEGF receptors (Table II). Among these, 28 (29.2%) cases were triple-VEGFR-negative, 22 cases (22.9%) were VEGFR1-predominant, 11 cases (11.5%) were triple-VEGFR-positive, and nine (9.4%) were VEGFR2-predominant.

VEGF receptor associations and clustering. Results of clustering analysis of the level of expression of VEGFR1, VEGFR2 and VEGFR3 in various histological subtypes of NSCLC cases are shown in Figure 4A. Based on differential expression of VEGFR2 and VEGFR3 in this cohort, (n=88) four distinct clusters were identified as follows: Cluster 1 (n=27, 30.7%) included cases with high vascular VEGFR2 and low or negative vascular VEGFR3 levels. Cluster 2 (n=16, 18.2%) cases were high in levels of both vascular VEGFR2 and VEGFR3. This cluster was dominated by squamous lung carcinoma histology. The largest cluster in this analysis was cluster 3 (n=40, 45.4%), which included cases that were low or negative both for VEGFR2 and VEGFR3 and dominated by ADC histology (Figure 4B). Although small, cluster 4 (n=5, 5.7%) included cases that showed high expression of VEGFR3 but were low or negative for VEGFR2.

Table II. *Proposed subclasses of non-small cell lung carcinoma (NSCLC) based on relative immunohistochemical (IHC) expression of vascular endothelial growth factor receptors VEGFR1, VEGFR2, and VEGFR3.*

Subclass of NSCLC by VEGFR IHC	VEGFR profile	No. of cases (%)
I	Triple-VEGFR-positive	11 (11.5)
II	VEGFR1-predominant	22 (22.9)
III	VEGFR2-predominant	9 (9.4)
IV	VEGFR3-predominant	3 (3.1)
V	Mixed, VEGFR1/2 predominant	13 (13.5)
VI	Mixed, VEGFR1/3 predominant	2 (2.1)
VII	Mixed, VEGFR2/3 predominant	8 (8.3)
VIII	Triple-VEGFR-low/negative	28 (29.2)
	Total cases	96 (100)

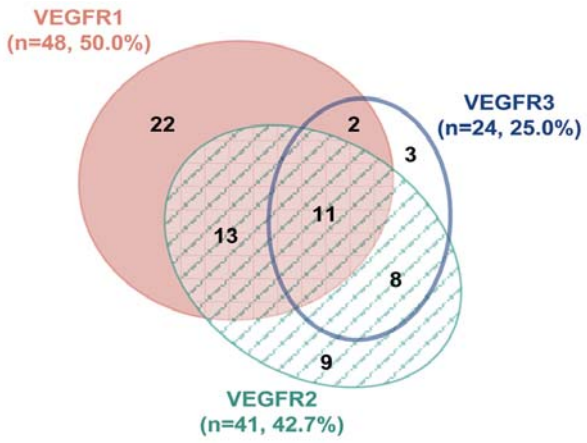

Figure 3. *Area-proportional 3-Venn diagram of vascular endothelial growth factor receptor (VEGFR) profiling in non-small cell lung carcinoma. Black numbers represent the number of cases that intersect between or among VEGFR1-, VEGFR2-, and VEGFR3-positive sets based on data described in Figure 2 and Table II.*

Associations between VEGFR IHC scores were determined. Categorical scores for VEGFR2 and VEGFR3 showed a positive association; a p-value of 0.0176 resulted from the chi-squared test for categorical data (Figure 4C), and $p<0.0001$ resulted from the correlation test for original continuous values. No association was observed between VEGFR1 and VEGFR2 (correlation test $p=0.5590$) or VEGFR1 and VEGFR3 (correlation test $p=0.8538$). Interestingly, most cases with moderate to high vascular VEGFR3 positivity also had similarly high expression of VEGFR2 (Figure 4D). Cases representing these four clusters are illustrated in Figure 5, which also includes relative expression of VEGFR1 in tumor cells in the NSCLC cases grouped in each of the four clusters.

Discussion

Recent advances in the treatment of NSCLC have been attributed to incremental progress in the understanding of it as a heterogeneous disease and include efforts to classify the disease into subtypes (26). Several anti-angiogenic agents are currently approved for the treatment of advanced NSCLC, including therapeutic antibodies and tyrosine-kinase inhibitors (TKIs). Both have led to increased progression-free survival in clinical trials of NSCLC, however, only the use of therapeutic monoclonal antibodies resulted in better overall survival (34), with the exception of the TKI nintedanib in combination with docetaxel (35). The large phase III trials that resulted in the approval of bevacizumab, a monoclonal antibody against VEGF (36, 37), and ramucirumab, a monocloncal antibody targeting VEGFR2 (38), were based on unselected patient populations. As characterization of the different patient populations that exist in NSCLC may depend on biomarker approaches that better represent complex angiogenesis signaling processes (12), we designed a biomarker approach that is amenable to clinical translation, as well as being informative on the design of pre-clinical studies: we characterized the relative expression of the prominent mediators of angiogenesis, the VEGFRs, to better understand the range and heterogeneity of expression in various histological subtypes of human NSCLC. We first characterized the relative VEGFR expression patterns and distribution in various human tissues (24, 25), and then applied these assessments to an archival cohort of primary NSCLC.

Our findings show immunoreactivity of VEGFR2 was localized to both the tumor vasculature and tumor cells, in line with findings in some recent studies (13, 24). In some of the recent publications using the same VEGFR2 antibody used in the current study (clone 55B11), VEGFR2 staining was reported to be localized only to tumor vasculature (19). Such a discrepancy may have a number of potential explanations as we and others have discussed previously (19, 24). Of note, 42.7% of NSCLC cases in our analysis were moderate to high for vascular expression of VEGFR2. This finding merits further investigation in larger, well-characterized series of NSCLC tissues.

VEGFR1 showed more widespread distribution in tumor cells, vessels, and inflammatory cells in the NSCLC tissues analyzed. Although we noted VEGFR1 expression in tumor vasculature, the overall intensity of VEGFR1 staining in tumor vasculature was not as high as in tumor cells. Not infrequently, the vascular expression of VEGFR1 was weak or focal, while tumor cell expression was generally diffuse. In addition, vascular expression of VEGFR1 did not correlate with the vascular expression of VEGFR2 or VEGFR3. In an IHC-based analysis, using polyclonal anti-

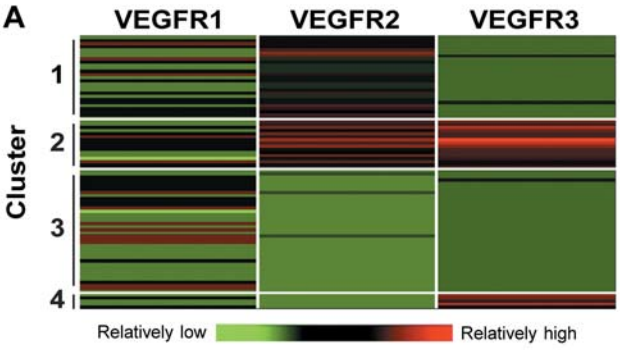

B

Cluster	ADC*	ADC w/lepidic pattern*	Large cell*	SCC*	Total
1	11	1	0	15	27
2	4	0	2	10	16
3	21	4	4	11	40
4	1	0	1	3	5

*Cases per cluster

C

		VEGFR1				VEGFR2		VEGFR3	
		N	L	M	H	+	-	+	-
VEGFR1	N	-	-	-	-	p = 0.6733		p = 0.2067	
	L	-	-	-	-				
	M	-	-	-	-				
	H	-	-	-	-				
VEGFR2	+	1	19	19	7	-	-	p = 0.0176	
	-	1	22	12	7	-	-		
VEGFR3	+	1	9	12	2	18	6	-	-
	-	1	32	19	12	28	36	-	-

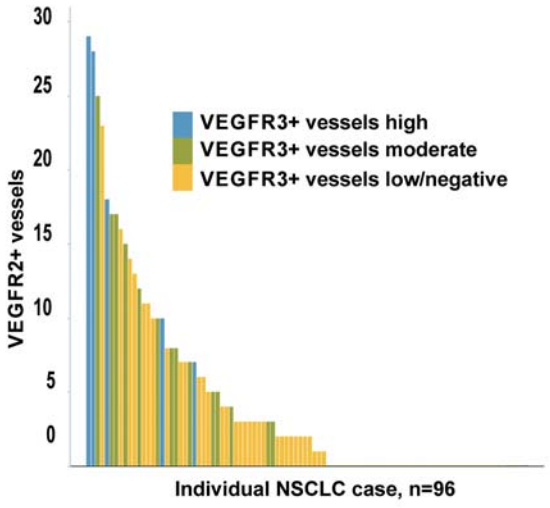

Figure 4. *Clustering and association analyses. A: K-means clustering analysis of vascular endothelial growth factor receptor (VEGFR) expression levels, on selected histologies (n=88). B: Number of positive cases in each cluster by histology (B). C: Correlation analysis results comparing each of the three VEGFRs to the others (categorical data). N, Negative for VEGFR1; L, low VEGFR1 expression; M, moderate VEGFR1 expression; H, high expression of VEGFR1. D: Bar graph of VEGFR2 vessel counts categorized by binned VEGFR3 vessel counts representing association of VEGFR2 and VEGFR3 as indicated in panel C, performed on all patients (n=96). ADC: adenocarcinoma; SCC: squamous cell carcinoma.*

VEGFR1 and monoclonal anti-VEGFR2, Decaussin et al. showed strong expression of both VEGFR1 and VEGFR2 in tumor cells, endothelial cells, and stromal fibroblasts, sometimes with membranous accentuation (18). These observations are in contrast to our findings and also to a previous report showing VEGF-induced angiogenesis requires an inverse regulation between VEGFR1 and VEGFR2 in tumor-associated endothelial cells (39). Interestingly, the anti-angiogenic effect of the anti-VEGF bevacizumab was shown to cause inverse reciprocal regulation of VEGFR1 and VEGFR2 expression levels in vascular endothelial cells in SCC (39), suggesting the relevance of systematic VEGFR profiling in this tumor type in the context of pathway inhibition.

In the current study, VEGFR3 was restricted to tumor vasculature, while Li et al. showed that VEGFR3 expression was localized to tumor cell cytoplasm and membrane with a frequency of 52.3% (21). Such discrepancy in prevalence of VEGFR3 may be due to different VEGFR3 assay conditions and their ability to detect distinct subcellular localization patterns of VEGFR3. In a recent IHC-based study on a cohort of 62 patients with NSCLC, 74.1% of cases were found to be positive for vascular expression of VEGFR2 and 64.5% for VEGFR3, respectively (20), much higher than in our study. Also previously reported, the percentages of patients with positive VEGFR expression in cancer cells were 100% for VEGFR2 and 77.4% for VEGFR3 (20). Such variation in prevalence and distribution of VEGFRs in different studies could be explained by differences in antibody selection and assay specificity, especially as the authors found all patients exhibited tumor cell staining of VEGFR2 and a majority of patients expressing VEGFR3 in the tumor epithelium. Such profound differences in the performance of various VEGFR assays highlight the need for technical verification of the results by standardized approaches including selection and demonstration of truly specific

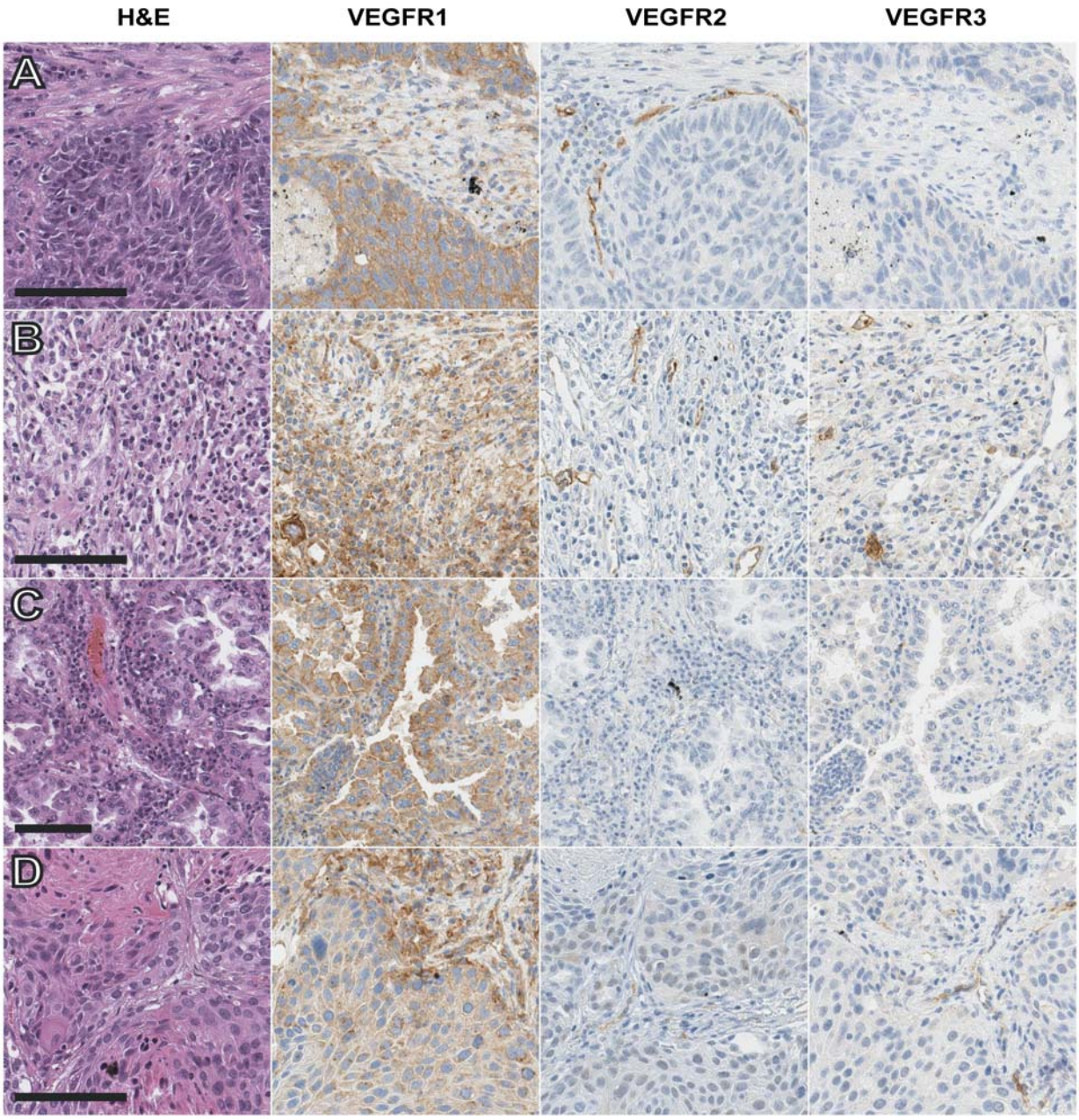

Figure 5. *Histomorphological and pathological findings of human non-small cell lung carcinoma. Images of Hematoxylin and Eosin stains and immunohistochemistry that are representative of cases in each cluster: squamous cell carcinoma (SCC), case 109, in cluster 1 (A); SCC, case 37, in cluster 2 (B); adenocarcinoma (ADC), case 96, in cluster 3 (C); and SCC, case 49, in cluster 4 (D). Slides were counterstained with hematoxylin (blue). Original magnification, ×200. Black bars=100 μm.*

antibodies, use of high-quality tissues, technically stringent assay optimization protocols, and careful interpretation of IHC staining results, as have been put forward over the years for standardization of IHC assays (40, 41).

The association between VEGFR2 and VEGFR3 expression in NSCLC is a finding that suggests communication between these receptors. Previous reports show VEGFR2 and VEGFR3 can heterodimerize and function to positively regulate angiogenic sprouting (42), and that they also must cooperate to promote lymphatic migration and proliferation (43). Additionally, in the absence of VEGFA, binding of VEGFC and VEGFD to VEGFR2 and

VEGFR3 may be sufficient to induce angiogenesis and tumor progression (44). It will be interesting to see if our VEGFR subclass VII (mixed, VEGFR2/3 predominant) is more responsive to inhibition of VEGFR2 or VEGFR3 than to inhibition of VEGFA ligand. This could be tested in relevant pre-clinical models of NSCLC.

In addition to manual selection of NSCLC cases in the form of various receptor-high or receptor-low subsets of cases, we also wanted to use an automated and objective method for clustering analysis of our VEGFR profiling. The clustering approach for various histological subtypes of NSCLC revealed four subsets of cases, of which the most important clusters were: cluster 2 (high in vascular VEGFR2 and VEGFR3), consisting predominantly of SCCs, and cluster 3 (low or negative for VEGFR2 and VEGFR3) comprising mainly ADC histology. These data also reveal interesting trends between relative expression of VEGFR2 and VEGFR3 in the tumor vasculature and histology of NSCLC. These findings are in line with analysis from Saintigny et al on a set of 92 NSCLC tissues in which 72% of VEGFR3-positive cases in the cohort were of squamous histology (22). Our observations regarding differential expression of VEGFR3 in various lung histologies are in line with those of Saintigny et al and could reasonably be corroborated with data from pertinent preclinical models, ideally those using various anti-angiogenic agents.

We recognize that limitations of our study include a relatively small NSCLC cohort. In addition, we did not include profiling of the expression of the various VEGF ligands, as soluble proteins produce a more diffuse staining pattern that is more challenging to score. We are investigating use of *in situ*-hybridization methods to more reliably report VEGF ligand expression. Moreover, it is clear that additional analytes will need to be added to our profiling panel to represent the contributions to angiogenic signaling by the platelet-derived growth factor receptors and fibroblast growth factor receptors (45). Finally, in our experience, IHC expression of the three VEGFRs was not uniform (monotonous) within a given NSCLC case, suggesting the frequent existence of intra-tumoral expression of the three VEGFRs in the NSCLC tissues analyzed. It will be interesting to see how the observed intra-tumoral heterogeneity of expression of the three VEGFRs will translate in future analyses of NSCLC, especially using conventional tissue sections.

While the characterization of NSCLC into subtypes has typically been based on genotype and histology (26), we propose that profiling of VEGFR protein expression by IHC may provide valuable understanding of disease heterogeneity in human NSCLC. We have already begun to test other tumor types in the same manner and observed some tumor-specific differences in relative expression of the three VEGFRs. For example, the NSCLC triple-VEGFR-negative subclass comprises one-third of the cases, while in CRC this subclass comprised only 3.6% of the cases (25). The unique VEGFR profiles in NSCLC compared with CRC suggest differences in VEGFR biology in these two cancer types, and raises the possibility that other human cancer types such as breast, gastric, and pancreatic cancer, may also exhibit unique VEGFR profiles.

We conclude that the heterogeneity of VEGFR profiles in NSCLC tissues represents some of the intricacies of angiogenic signaling and that the proposed subclasses of NSCLC are an approach to complement lines of investigation beginning with systematic characterization of the disease. These observations allow for the formation of data-driven hypotheses to test the status of pathological angiogenesis in human NSCLC as well as relevant pre-clinical tumor models. For instance, one can hypothesize that tumor model tissues that exhibit high levels of all three receptors (triple-VEGFR-positive) or VEGFR2 and VEGFR3 (VEGFR2/VEGFR3-predominant) may respond differently to anti-angiogenic treatment as compared to those which lack all three VEGFRs (triple-VEGFR-negative). We are currently investigating the link between IHC-based VEGFR subclasses and canonical pathways involved in proliferation, survival, angiogenesis, and metastasis using gene expression profiling.

Acknowledgements

The Authors gratefully acknowledge expert pathology support from Kelly Credille, DVM, Ph.D., Dip. ACVP, as well as the Experimental Pathology Laboratory scientists and histotechnologists at Eli Lilly and Company. Appreciation goes to Ashley Bay and Amanda Estelle (Lilly) for work on *in situ* hybridization. Thanks to Karen Yamamoto, Ph.D. (Clarient) for support on IHC, and to Yuewei Qian, Ph.D. and Xiaohua Huanghe (Lilly) for generating recombinant protein. They also recognize Milan Bhagat (TriStar) for critical support of TMA sample and patient data.

References

1 Folkman J: Role of angiogenesis in tumor growth and metastasis. Semin Oncol *29*: 15-18, 2002.

2 Carmeliet P and Jain RK: Molecular mechanisms and clinical applications of angiogenesis. Nature *473*: 298-307, 2011.

3 Piperdi B, Merla A and Perez-Soler R: Targeting angiogenesis in squamous non-small cell lung cancer. Drugs *74*: 403-413, 2014.

4 McGuire S: World Cancer Report 2014. Geneva, Switzerland: World Health Organization, International Agency for Research on Cancer, WHO Press, 2015. Adv Nutr *7*: 418-419, 2016.

5 Novello S, Kaiser R, Mellemgaard A, Douillard JY, Orlov S, Krzakowski M, von Pawel J, Gottfried M, Bondarenko I, Liao M, Barrueco J, Gaschler-Markefski B, Griebsch I, Palmer M and Reck M: Analysis of patient-reported outcomes from the LUME-Lung 1 trial: a randomised, double-blind, placebo-controlled, Phase III study of second-line nintedanib in patients with advanced non-small cell lung cancer. Eur J Cancer *51*: 317-326, 2015.

6 Ellis PM and Al-Saleh K: Multitargeted anti-angiogenic agents and NSCLC: clinical update and future directions. Crit Rev Oncol/Hematol *84*: 47-58.

7 Zaba O, Grohe C and Merk J: Novel therapies in non-small cell lung cancer. Minerva Chir *66*: 235-244, 2011.

8 Das M and Wakelee H: Angiogenesis and lung cancer: ramucirumab prolongs survival in 2nd-line metastatic NSCLC. Transl Lung Cancer Res *3*: 397-399, 2014.

9 Masago K, Fujimoto D, Fujita S, Hata A, Kaji R, Ohtsuka K, Okuda C, Takeshita J, and Katakami N: Response to bevacizumab combination chemotherapy of malignant pleural effusions associated with non-squamous non-small-cell lung cancer. Mol Clin Oncol *3*: 415-419, 2015.

10 Larsen JE and Minna JD: Molecular biology of lung cancer: clinical Implications. Clin Chest Med *32*: 703-740, 2011.

11 Alberg AJ and Samet JM: Epidemiology of lung cancer. Chest *123*: 21S-49S, 2003.

12 Pilotto S, Bonomi M, Massari F, Milella M, Ciuffreda L, Brunelli M, Fassan M, Chilosi M, Scarpa A, Tortora G and Bria E: Anti-angiogenic drugs and biomarkers in non-small-cell lung cancer: a 'hard days night'. Curr Pharm Des *20*: 3958-3972, 2014.

13 Goel HL and Mercurio AM: VEGF targets the tumour cell. Nat Rev Cancer *13*: 871-882, 2013.

14 Shibuya M: VEGFR and type-V RTK activation and signaling. Cold Spring Harb Perspect Biol *5*: a009092, 2013.

15 Ferrara N, Gerber HP, and LeCouter J: The biology of VEGF and its receptors. Nat Med *9*: 669-676, 2003.

16 Karkkainen MJ and Petrova TV: Vascular endothelial growth factor receptors in the regulation of angiogenesis and lymphangiogenesis. Oncogene *19*: 5598-5605, 2000.

17 Donnem T, Al-Shibli K, Al-Saad S, Delghandi MP, Busund LT, and Bremnes RM: VEGF-A and VEGFR-3 correlate with nodal status in operable non-small cell lung cancer: inverse correlation between expression in tumor and stromal cells. Lung Cancer *63*: 277-283, 2009.

18 Decaussin M, Sartelet H, Robert C, Moro D, Claraz C, Brambilla C and Brambilla E: Expression of vascular endothelial growth factor (VEGF) and its two receptors (VEGF-R1-FLT1 and VEGF-R2-FLK1/KDR) in non-small cell lung carcinomas (NSCLCs): correlation with angiogenesis and survival. J Pathol *188*: 369-377, 1999.

19 Smith NR, Baker D, James NH, Ratcliffe K, Jenkins M, Ashton SE, Sproat G, Swann R, Gray N, Ryan A, Jurgensmeier JM and Womack C: Vascular endothelial growth factor receptors VEGFR-2 and VEGFR-3 are localized primarily to the vasculature in human primary solid cancers. Clin Cancer Res *16*: 3548-3561, 2010.

20 Kajita T, Ohta Y, Kimura K, Tamura M, Tanaka Y, Tsunezuka Y, Oda M, Sasaki T and Watanabe G: The expression of vascular endothelial growth factor C and its receptors in non-small cell lung cancer. Br J Cancer *85*: 255-260, 2001.

21 Li J, Hong M and Pan T: Clinical significance of VEGF-C and VEGFR-3 expression in non-small cell lung cancer. J Huazhong Univ Sci Technolog Med Sci *26*: 587-590, 2006.

22 Saintigny P, Kambouchner M, Ly M, Gomes N, Sainte-Catherine O, Vassy R, Czernichow S, Letoumelin P, Breau JL, Bernaudin JF and Kraemer M: Vascular endothelial growth factor-C and its receptor VEGFR-3 in non-small-cell lung cancer: concurrent expression in cancer cells from primary tumour and metastatic lymph node. Lung Cancer *58*: 205-213, 2007.

23 Zheng CL, Qiu C, Shen MX, Qu X, Zhang TH, Zhang JH and Du JJ: Prognostic impact of elevation of vascular endothelial growth factor family expression in patients with non-small cell lung cancer: an updated meta-analysis. Asian Pac J Cancer Prev *16*: 1881-1895, 2015.

24 Holzer TR, Fulford AD, Nedderman DM, Umberger TS, Hozak RR, Joshi A, Melemed SA, Benjamin LE, Plowman GD, Schade AE, Ackermann BL, Konrad RJ and Nasir A: Tumor cell expression of vascular endothelial growth factor receptor 2 is an adverse prognostic factor in patients with squamous cell carcinoma of the lung. PLoS ONE *8*: e80292, 2013.

25 Nasir A, Reising LO, Nedderman DM, Fulford AD, Uhlik MT, Benjamin LE, Schade AE and Holzer TR: Heterogeneity of vascular endothelial growth factor receptors 1, 2, 3 in primary human colorectal carcinoma. Anticancer Res *36*: 2683-2696, 2016.

26 Thomas A, Liu SV, Subramaniam DS and Giaccone G: Refining the treatment of NSCLC according to histological and molecular subtypes. Nat Rev Clin Oncol *12*: 511-526, 2015.

27 Beasley MB, Brambilla E and Travis WD: The 2004 World Health Organization classification of lung tumors. Semin Roentgenol *40*: 90-97, 2005.

28 Travis WD, Brambilla E, Nicholson AG, Yatabe Y, Austin JH, Beasley MB, Chirieac LR, Dacic S, Duhig E, Flieder DB, Geisinger K, Hirsch FR, Ishikawa Y, Kerr KM, Noguchi M, Pelosi G, Powell CA, Tsao MS, Wistuba I and Panel WHO: The 2015 World Health Organization classification of lung tumors: impact of genetic, clinical and radiologic advances since the 2004 classification. J Thorac Oncol *10*: 1243-1260, 2015.

29 Holzer TR, Nedderman DM and Nasir A: Abstract 4175: Robust immunohistochemical assay to characterize human cancer tissues for prevalence of vascular endothelial growth factor receptor 3 (VEGFR3). Cancer Res *75*: 4175-4175, 2015.

30 Chu AY, Litzky LA, Pasha TL, Acs G and Zhang PJ: Utility of D2-40, a novel mesothelial marker, in the diagnosis of malignant mesothelioma. Mod Pathol *18*: 105-110, 2005.

31 Ramani P, Bradley NJ and Fletcher CD: QBEND/10, a new monoclonal antibody to endothelium: assessment of its diagnostic utility in paraffin sections. Histopathology *17*: 237-242, 1990.

32 Micallef L and Rodgers P: eulerAPE: drawing area-proportional 3-Venn diagrams using ellipses. PLoS ONE *9*: e101717, 2014.

33 Petrova TV, Bono P, Holnthoner W, Chesnes J, Pytowski B, Sihto H, Laakkonen P, Heikkila P, Joensuu H and Alitalo K: VEGFR-3 expression is restricted to blood and lymphatic vessels in solid tumors. Cancer Cell *13*: 554-556, 2008.

34 Hong S, Tan M, Wang S, Luo S, Chen Y and Zhang L: Efficacy and safety of angiogenesis inhibitors in advanced non-small cell lung cancer: a systematic review and meta-analysis. J Cancer Res Clin Oncol *141*: 909-921, 2015.

35 Noonan S, Man Wong K and Jimeno A: Nintedanib, a novel triple angiokinase inhibitor for the treatment of non-small cell lung cancer. Drugs Today (Barc) *51*: 357-366, 2015.

36 Reck M, von Pawel J, Zatloukal P, Ramlau R, Gorbounova V, Hirsh V, Leighl N, Mezger J, Archer V, Moore N and Manegold C: Phase III trial of cisplatin plus gemcitabine with either placebo or bevacizumab as first-line therapy for nonsquamous non-small-cell lung cancer: AVAil. J Clin Oncol *27*: 1227-1234, 2009.

37 Su Y, Yang WB, Li S, Ye ZJ, Shi HZ and Zhou Q: Effect of angiogenesis inhibitor bevacizumab on survival in patients with cancer: a meta-analysis of the published literature. PLoS ONE *7*: e35629, 2012.

38 Garon EB, Ciuleanu TE, Arrieta O, Prabhash K, Syrigos KN, Goksel T, Park K, Gorbunova V, Kowalyszyn RD, Pikiel J, Czyzewicz G, Orlov SV, Lewanski CR, Thomas M, Bidoli P, Dakhil S, Gans S, Kim JH, Grigorescu A, Karaseva N, Reck M, Cappuzzo F, Alexandris E, Sashegyi A, Yurasov S and Perol M: Ramucirumab plus docetaxel *versus* placebo plus docetaxel for second-line treatment of stage IV non-small-cell lung cancer after disease progression on platinum-based therapy (REVEL): a multicentre, double-blind, randomised phase 3 trial. Lancet *384*: 665-673, 2014.

39 Zhang Z, Neiva KG, Lingen MW, Ellis LM and Nor JE: VEGF-dependent tumor angiogenesis requires inverse and reciprocal regulation of VEGFR1 and VEGFR2. Cell Death Differ *17*: 499-512, 2010.

40 Bordeaux J, Welsh A, Agarwal S, Killiam E, Baquero M, Hanna J, Anagnostou V and Rimm D: Antibody validation. Biotechniques *48*: 197-209, 2010.

41 Ramos-Vara JA and Miller MA: When tissue antigens and antibodies get along: revisiting the technical aspects of immunohistochemistry – the red, brown, and blue technique. Vet Pathol *51*: 42-87, 2014.

42 Nilsson I, Bahram F, Li X, Gualandi L, Koch S, Jarvius M, Soderberg O, Anisimov A, Kholova I, Pytowski B, Baldwin M, Yla-Herttuala S, Alitalo K, Kreuger J and Claesson-Welsh L: VEGF receptor 2/-3 heterodimers detected *in situ* by proximity ligation on angiogenic sprouts. EMBO J *29*: 1377-1388, 2010.

43 Goldman J, Rutkowski JM, Shields JD, Pasquier MC, Cui Y, Schmokel HG, Willey S, Hicklin DJ, Pytowski B and Swartz MA: Cooperative and redundant roles of VEGFR-2 and VEGFR-3 signaling in adult lymphangiogenesis. FASEB J *21*: 1003-1012, 2007.

44 Clarke JM and Hurwitz HI: Understanding and targeting resistance to anti-angiogenic therapies. J Gastrointest Oncol *4*: 253-263, 2013.

45 Kono SA, Heasley LE, Doebele RC and Camidge DR: Adding to the mix: fibroblast growth factor and platelet-derived growth factor receptor pathways as targets in non–small cell lung cancer. Curr Cancer Drug Targets *12*: 107-123, 2012.

46 Greene FL, Page DL, Fleming ID, Fritz AG, Balch CM, Haller DG and Morrow M (eds.): AJCC Cancer Staging Manual. Chicago, Springer, pp. 167-177, 2006.

Received April 13, 2016
Revised May 26, 2016
Accepted May 31, 2016